



CHORUS

This is the accepted manuscript made available via CHORUS. The article has been published as:

Secondary Magnetic Islands Generated by the Kelvin-Helmholtz Instability in a Reconnecting Current Sheet

R. L. Fermo, J. F. Drake, and M. Swisdak

Phys. Rev. Lett. **108**, 255005 — Published 20 June 2012

DOI: [10.1103/PhysRevLett.108.255005](https://doi.org/10.1103/PhysRevLett.108.255005)

Secondary magnetic islands generated by the Kelvin-Helmholtz instability in a reconnecting current sheet

R. L. Fermo

Center for Space Physics, Astronomy Department, Boston University, Boston, MA 02215, USA

J. F. Drake and M. Swisdak

*Institute for Research in Electronics and Applied Physics, Department of Physics,
University of Maryland, College Park, MD 20742-3511, USA*

(Dated: April 27, 2012)

Magnetic islands or flux ropes produced by magnetic reconnection have been observed on the magnetopause, in the magnetotail, and in coronal current sheets. Particle-in-cell (PIC) simulations of magnetic reconnection with a guide field produce elongated electron current layers that spontaneously produce secondary islands. Here, we explore the seed mechanism that gives birth to these islands. The most commonly suggested theory for island formation is the tearing instability. We demonstrate that in our simulations these structures typically start out, not as magnetic islands, but as electron flow vortices within the electron current sheet. When some of these vortices first form, they do not coincide with closed magnetic field lines, as would be the case if they were islands. Only after they have grown larger than the electron skin depth do they couple to the magnetic field and seed the growth of finite-sized islands. The streaming of electrons along the magnetic separatrix produces the flow shear necessary to drive an electron-Kelvin-Helmholtz instability and produce the initial vortices. The conditions under which this instability is the dominant mechanism for seeding magnetic islands are explored.

PACS numbers: 52.35.Vd,94.30.cp,96.60.Iv

Current sheets undergoing patchy magnetic reconnection result in the formation of magnetic islands, or flux ropes in 3-D. Theoretically, a linear magnetohydrodynamic (MHD) treatment of a current layer predicts that the tearing instability will produce multiple x-lines (and subsequently magnetic islands) for long wavelength perturbations, $kw \lesssim 1$, where k is the wavenumber and w the current sheet thickness [1]. Observationally, the presence of these structures has been inferred in the magnetopause [2, 3], the magnetotail [4–7], and coronal current sheets [8–10]. Islands appear in MHD simulations with sufficiently high Lundquist number [11–14] and in particle-in-cell (PIC) simulations [15–20].

Recent interest in magnetic islands can be attributed to their connection with particle energization (via the Fermi mechanism [21]) and enhanced reconnection rates. Although Sweet-Parker reconnection [22] is far too slow to explain the energy release in solar flares, a rescaling of Sweet-Parker that accounts for the presence of magnetic islands would enhance the reconnection rate by \sqrt{N} , where N is the number of islands [13]. However, for coronal parameters, a Sweet-Parker analysis predicts that the current sheet will thin between islands to less than an ion inertial length, $d_i = c/\omega_{pi}$, prior to the onset of fast reconnection. At this point, the transition to kinetic scales triggers Hall physics [23], which enables fast reconnection to onset [24]. A complete theory of magnetic islands should therefore include kinetic scales as well as macroscales [25, 26]. A better understanding of the generation mechanism for magnetic islands is hence highly desirable, and has been explored in other recent literature in the MHD limit [15, 20, 27, 28]. In this paper, we are interested in island formation after fast reconnection has onset [29].

To this end, we return to the simulations performed by Drake et al. [15]. In those simulations, reconnection with a guide field led to elongated electron current sheets, within which secondary islands developed. We perform similar simulations at higher resolution to investigate how these secondary islands first form at scales of the electron skin depth. The 2D simulations were performed using the PIC code P3D, which evolves the electromagnetic field using the full Maxwell equations and steps particles forward using the Lorentz force law [30]. In our simulations, space and time are normalized to d_i and the ion cyclotron period Ω_{ci}^{-1} . In these units, velocity is normalized to the upstream Alfvén speed c_A , and we choose $c = 15$, and $m_i/m_e = 25$. The simulation domain is $L_x \times L_y = 102.4d_i \times 51.2d_i$ with periodic boundary conditions, using 8192×4096 cells, ensuring that we comfortably resolve the electron skin depth $d_e = 0.2d_i$. The time step is $0.0025\Omega_{ci}^{-1}$. The initial configuration is a pair of Harris sheets [31] of width $w_0 = d_i$ with a reversing magnetic field $B_0 = 1.0$ and a uniform guide field $B_g = 2B_0$. A magnetic field perturbation in each current sheet produces x-lines at $(L_x/4, 3L_y/4)$ and $(3L_x/4, L_y/4)$, which yields a single primary magnetic island on each current sheet. An ambient background density of $0.2n_0$ supplements the Harris sheet density necessary to maintain pressure balance. The initial velocity distributions are Maxwellian, but in order to explore a range of temperatures, we perform two simulations, with $T_i/T_e = 0.25$ and $T_i/T_e = 4$, and $T_e + T_i = 0.5$ to balance the external magnetic pressure. Both values for the temperature ratio produced similar results.

Just as in the simulations of guide field reconnection by Drake et al. (2006) [15], our simulation produced a tilted electron current sheet along the separatrices. These current layers elongate and the single x-line perturbation becomes unstable to the formation of secondary islands. In Drake et al. (2006), the creation of secondary islands was attributed to the tearing instability, citing that $k \sim 4.0d_i^{-1}$ and $w \sim 0.13d_i$ such that $kw \sim 0.5 < 1$. This is in accord with most of the present literature based on MHD theory [1, 27, 32], MHD simulations [28], 2-D PIC simulations without a guide field [16, 17, 19], and most recently, in 3-D reconnection simulations [20].

However, we consider here whether a different mechanism is responsible for the generation of magnetic islands. The impetus for such a consideration is illustrated in Fig. 1, which shows one such secondary magnetic island that formed in the electron current sheet in the $T_i/T_e = 4$ simulation. The structure appears to be a simple magnetic island in Fig. 1(a), but a closer inspection reveals a surprising feature: vortical electron flows around and within the island. In Fig. 1(b), we see similarities to Kelvin-Helmholtz vortices associated with shear flows.

We posit that the structure in Fig. 1 started out not as a magnetic island, but as a Kelvin-Helmholtz vortex. To demonstrate this, we follow a single magnetic island from its birth in the electron current sheet until its expulsion from the x-line region into the primary magnetic island. The island shown in Fig. 1 was born very close to the primary x-line around $4\Omega_{ci}^{-1}$ prior to the time shown. For this reason, the island continued to grow for some time without convecting away from the x-line. However, having been born so close to the primary x-line, it would be difficult to distinguish a reconnection site that develops out of the tearing mode from the primary x-line of the system.

A more useful case to study, then, is an island that was born along the tilted electron current sheet slightly away from the primary x-line, where it might be easier to distinguish a fluid flow instability from a tearing instability. The $T_i/T_e = 0.25$ case, having higher electron temperature, produces a slightly thicker electron current sheet. In both cases, the resulting magnetic islands at late times exhibit the vortical flows consistent with generation by a Kelvin-Helmholtz instability. For illustrative purposes though, the $T_i/T_e = 0.25$ case is preferable because the electron current sheet is better resolved, enabling a clearer picture of the internal structure of the islands which form within it.

In particular, we observe an island along the tilted electron current sheet that started out quite small in Fig. 2(a),

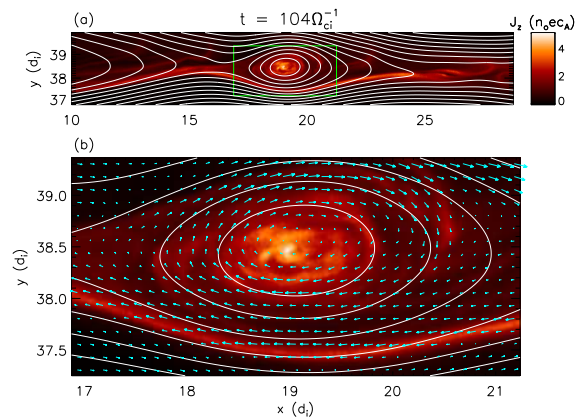


FIG. 1. (a) The out-of-plane current density J_z and contours of the magnetic field near the x-line at $t = 104\Omega_{ci}^{-1}$ in the $T_i/T_e = 4$ simulation. (b) A zoom-in of the region within the green box of (a), with arrows showing the electron flow in the frame of the mean electron outflow $\mathbf{v}_e + c_A \hat{\mathbf{x}}$.

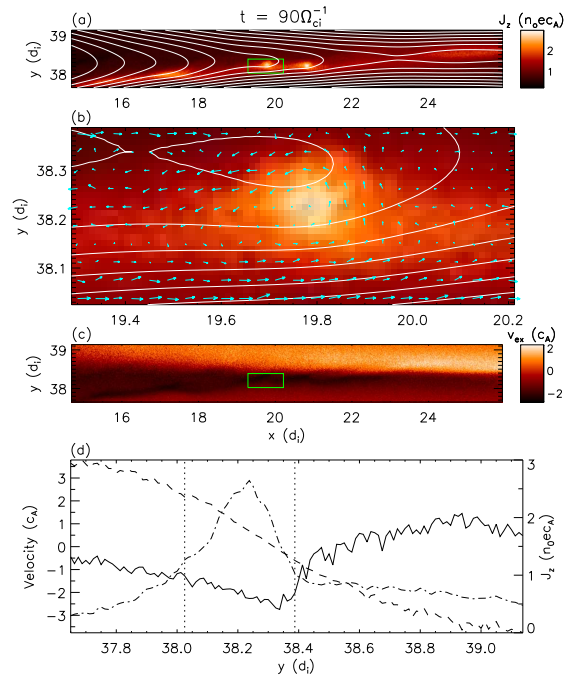


FIG. 2. (a) The out-of-plane current density J_z and contours of the magnetic field near the x-line at $t = 90\Omega_{ci}^{-1}$ in the $T_i/T_e = 0.25$ simulation. (b) A zoom-in of the region within the green box of (a), with arrows showing the electron flow in the frame of the electron outflow, $\mathbf{v}_e + 2c_A \hat{\mathbf{x}}$. (c) The reconnection electron outflow v_{ex} . (d) Vertical cuts of v_{ex} (solid curve), $c_{Aex}/2$ (dashed curve), and J_z (dash-dotted curve, on the right axis) through the center of the green box in (c), with dashed vertical lines denoting the top and bottom boundaries of the green box.

at the scale of the electron skin depth $d_e = 0.2d_i$, and $\sim 5d_i$ away from the primary x-line. Note in Fig. 2(b) – corresponding to the region encompassed by the green box in Fig. 2(a) – that the J_z enhancement induces a magnetic island structure, but the two are not colocated. At this scale within the electron current layer, the J_z enhancement is still mostly decoupled from the magnetic field. In fact, because the current sheet is tilted along the separatrix, it is not close enough to the magnetic field reversal region to trigger the tearing instability. The magnetic island, by its very nature, must form at the reversal region and not at the electron current sheet.

A closer examination of the electron flow within the current sheet corroborates this story. If the tearing instability were responsible for the generation of the magnetic island in Fig. 2(b), we should expect vertical inflows on either side of the island, and horizontal outflows from a reconnection site, as illustrated in Fig. 3. On the contrary, Fig. 2(b) shows

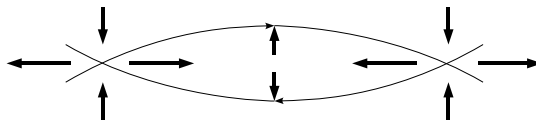


FIG. 3. Expected flow profile for an island produced by a tearing instability.

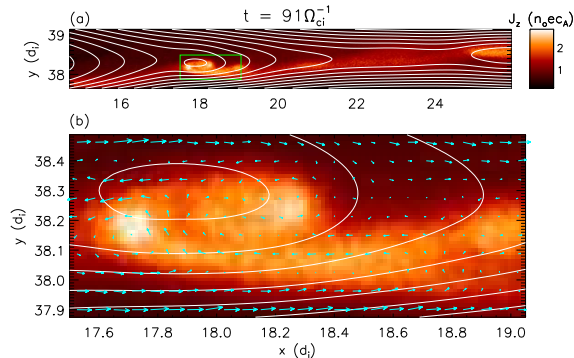


FIG. 4. Same format as Fig. 2(a)-(b) at $t = 91\Omega_{ci}^{-1}$.

that (after transforming into the frame of the electron outflow from the primary reconnection x-line $\mathbf{v}_e = -2c_A\hat{\mathbf{x}}$) the electrons at this very early stage exhibit vortical flows, more consistent with a Kelvin-Helmholtz vortex than with a magnetic island generated by the tearing mode. There is no discernible inflow or corresponding outflow near the x-line to the left of the magnetic island, nor any current enhancement at this location.

To verify that conditions are favorable for the Kelvin-Helmholtz instability, Fig. 2(c) shows v_{ex} in the vicinity of this structure. Because it exists near the separatrix, there is a sharp velocity gradient across the current sheet from $v_{ex} \approx 0$ outside of the separatrix to $v_{ex} \approx -2c_A$ within the reconnection exhaust. The velocity shear is shown clearly in a vertical cut of v_{ex} , Fig. 2(d), along with the out-of-plane current density. The vortex forms in the vicinity of the strongest velocity shear combined with the largest current density. Generally, the velocity shear must also overcome any stabilizing effects from a magnetic field in the direction of streaming associated with Alfvén waves [33] or whistler waves. For the electron Kelvin-Helmholtz instability to develop within a current sheet of thickness d_e , the characteristic growth rate $\gamma \sim \Delta v_{ex}/d_e$ must exceed the whistler frequency

$$\omega \sim \Omega_{cex} \frac{k^2 d_e^2}{1 + k^2 d_e^2}. \quad (1)$$

Taking $k \sim 1/d_e$, we obtain the instability criterion

$$\Delta v_{ex} > \frac{c_{Aex}}{2} \quad (2)$$

where $c_{Aex} = B_x/\sqrt{4\pi m_e n}$ is the electron Alfvén speed based on the local horizontal magnetic field, which drops in magnitude close to the current sheet. The dashed line in Fig. 2(d) shows that $|c_{Aex}|/2 \lesssim 2$ in the vicinity of the vortex, consistent with the instability criterion in Eq. (2).

As the vortex flows away from the x-line, the current J_z entrapped in the vortex grows, as seen in Fig. 4. This growth is due to plasma flowing out from the primary x-line and piling up at the vortex. Although the vortex is itself flowing outwards, plasma accelerated by E_{\parallel} streams along the current sheet and accumulates in the vortex in Fig. 4(a). Another source of growth is that by $t = 91\Omega_{ci}^{-1}$, a vortex that was born slightly upstream of the vortex observed in Fig. 2 has collided with it, and the two are now spiraling around one another in Fig. 4(b). The vortex has now grown larger than d_e , and consequently is now beginning to recouple to the magnetic field in Fig. 4(a) as the surrounding magnetic field gets swept up into the vortex.

In Fig. 5(a), the coupling to the magnetic field has progressed even further so that the structure appears to be a true magnetic island (albeit off-center from the J_z enhancement). With the electrons now recoupled to the magnetic field, growth by the Kelvin-Helmholtz instability may be inhibited, but at this point, island growth can be driven by other factors (electron streaming along the current sheet, merging, and potentially even reconnection) independently

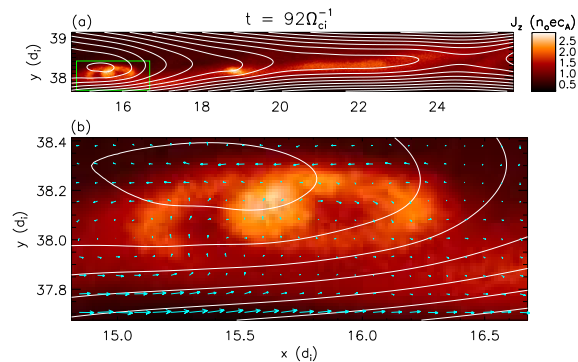


FIG. 5. Same format as Fig. 2(a)-(b) at $t = 92\Omega_{ci}^{-1}$.

of Kelvin-Helmholtz. Fig. 5(b) shows that the vortical flows have remained intact, even though it is no longer a single coherent vortex. Unfortunately, we are not able to follow this particular structure much further because by now it has been ejected and is starting to interact with the downstream magnetic field. Although we see the beginnings of a secondary magnetic island here, in general the electron Kelvin-Helmholtz vortex must begin close enough to the reversal surface and have enough time to outgrow the electron current sheet in order to form a true magnetic island. Fig. 1 showed one such case where the flow vortex persisted for quite a long time (at least $10\Omega_{ci}^{-1}$) in an island that remained largely stationary. The online auxiliary material includes a video of the growth of vortices into magnetic islands, which illustrates very clearly the vortical flow within these islands.

Once the tilted electron current sheet forms, the electron Kelvin-Helmholtz instability, and not the tearing instability, is the dominant mechanism for secondary island formation, at least in these simulations and in several others of component reconnection [15]. This mechanism is effective for a range of guide fields (for $B_g = 2B_0$ here, and for $B_g = B_0$ in Drake et al. [15], so long as the guide field generates the tilted electron current sheet) as well as a wide range of temperatures ($T_i/T_e = 0.25$ to $T_i/T_e = 4$). The $T_i/T_e = 4$ case is more representative of magnetospheric plasma and suggests that island generation by the Kelvin-Helmholtz instability is viable there. Once the initial vortex has matured into a true magnetic island, continued island growth can be driven by reconnection. However, the role of the Kelvin-Helmholtz instability as the original seed for island formation is evident even in relatively large islands such as in Fig. 1 which still exhibit vortical flow. Thus, even the larger islands are initially generated at electron skin depth scales $d_e = c/\omega_{pe}$. Consequently, in narrow current layers, neither linear MHD theories of plasmoid formation nor MHD simulations will fully describe magnetic islands early in their development. Although the islands formed in this way start out quite small, in large systems such as those in the corona and magnetosphere, their sheer number and lengthy transit time might allow them to grow into macroscale objects which affect global dynamics [25, 26].

This work was supported by NASA through an Earth and Space Science Fellowship NNX07A083H and NNX09A102G. Computations were performed at the National Energy Research Scientific Computing Center.

-
- [1] H. P. Furth, J. Killeen, and M. N. Rosenbluth, *Phys. Fluids* **6**, 459 (April 1963).
- [2] C. T. Russell and R. C. Elphic, *Geophys. Res. Lett.* **6**, 33 (1979).
- [3] C. J. Farrugia, R. P. Rijnbeek, M. A. Saunders, D. J. Southwood, D. J. Rodgers, M. F. Smith, C. P. Chaloner, D. S. Hall, P. J. Christiansen, and L. J. C. Woolliscroft, *J. Geophys. Res.* **93**, 14465 (1988).
- [4] E. W. Hones, Jr., D. N. Baker, S. J. Bame, W. C. Feldman, J. T. Gosling, D. J. McComas, R. D. Zwickl, J. A. Slavin, E. J. Smith, and B. T. Tsurutani, *Geophys. Res. Lett.* **11**, 5 (1984).
- [5] J. A. Slavin, M. F. Smith, E. L. Mazur, D. N. Baker, E. W. Hones, Jr., T. Iyemori, and E. W. Greenstadt, *J. Geophys. Res.* **98**, 15425 (1993).
- [6] J. A. Slavin, R. P. Lepping, J. Gjerloev, D. H. Fairfield, M. Hesse, C. J. Owen, M. B. Moldwin, T. Nagai, A. Ieda, and T. Mukai, *J. Geophys. Res.* **108**, 1015 (2003).
- [7] J. P. Eastwood, T.-D. Phan, F. S. Mozer, M. A. Shay, M. Fujimoto, A. Retin, M. Hesse, A. Balogh, E. A. Lucek, and I. Dandouras, *J. Geophys. Res.* **112**, A06235 (2007).
- [8] D. E. McKenzie and H. S. Hudson, *Ap. J.* **519**, L93 (2009).
- [9] N. R. Sheeley, H. P. Warren, and Y.-M. Wang, *Astrophys. J.* **616**, 1224 (2004).
- [10] M. G. Linton and D. W. Longcope, *Ap. J.* **642**, 1177 (2006).
- [11] D. Biskamp, *Phys. Fluids* **29**, 1520 (1986).
- [12] G. Lapenta, *Phys. Rev. Lett.* **100**, 235001 (2008).
- [13] P. A. Cassak, M. A. Shay, and J. F. Drake, *Phys. Plasmas* **16**, 120702 (2009).
- [14] Y.-M. Huang and A. Bhattacharjee, *Phys. Plasmas* **17**, 062104 (2010).
- [15] J. F. Drake, M. Swisdak, K. M. Schoeffler, B. N. Rogers, and S. Kobayashi, *Geophys. Res. Lett.* **33**, L13105 (2006).
- [16] W. Daughton, H. Karimabadi, and J. Scudder, *Phys. Plasmas* **13**, 072101 (2006).
- [17] K. Fujimoto, *Phys. Plasmas* **13**, 072904 (2006).
- [18] H. Karimabadi, W. Daughton, and J. Scudder, *Geophys. Res. Lett.* **34**, L13104 (2007).
- [19] A. Klimas, M. Hesse, and S. Zenitani, *Phys. Plasmas* **15**, 082102 (2008).
- [20] W. Daughton, V. Roytershteyn, H. Karimabadi, L. Yin, B. J. Albright, B. Bergen, and K. J. Bowers, *Nature Phys.* **7**, 539 (2011).
- [21] J. F. Drake, M. Swisdak, H. Che, and M. A. Shay, *Nature* **443**, 553 (2006).
- [22] P. A. Sweet, in *Electromagnetic Phenomena in Cosmical Physics*, edited by B. Lehnert (Cambridge University Press, New York, 1958) p. 123.
- [23] W. Daughton, V. Roytershteyn, B. J. Albright, H. Karimabadi, L. Yin, and K. J. Bowers, *Phys. Rev. Lett.* **103**, 065004 (2009).
- [24] M. A. Shay, J. F. Drake, and M. Swisdak, *Phys. Rev. Lett.* **99**, 155002 (2007).
- [25] R. L. Fermo, J. F. Drake, and M. Swisdak, *Phys. Plasmas* **17**, 010702 (2010).
- [26] R. L. Fermo, J. F. Drake, M. Swisdak, and K.-J. Hwang, *J. Geophys. Res.*, A09226(2011).
- [27] N. F. Loureiro, A. A. Schekochihin, and S. Cowley, *Phys. Plasmas* **14**, 100703 (2007).
- [28] R. Samtaney, N. F. Loureiro, D. A. Uzdensky, A. A. Schekochihin, and S. C. Cowley, *Phys. Rev. Lett.* **103**, 105004 (2009).
- [29] R. L. Fermo, *Magnetic islands produced by reconnection in large current layers: A statistical approach to modeling at global scales*, Ph.D. thesis, University of Maryland (2011).
- [30] A. Zeiler, D. Biskamp, J. F. Drake, B. N. Rogers, M. A. Shay, and M. Scholer, *J. Geophys. Res.* **107**, 1230 (2002).
- [31] E. G. Harris, *Nuovo Cim.* **23**, 115 (1962).
- [32] S. V. Bulanov, S. I. Syrovatskii, and J. Sakai, *Pis'ma Zh. Eksp. Teor. Fiz.* **28**, 177 (1978).
- [33] S. Chandrasekhar, *Hydrodynamic and Hydromagnetic Stability* (Dover Publications, New York, 1961).